ELSEVIER

Journal of Molecular Catalysis A: Chemical 182–183 (2002) 47–60

JOURNAL OF MOLECULAR CATALYSIS A: CHEMICAL

www.elsevier.com/locate/molcata

Carbon-supported iridium catalysts in the catalytic wet air oxidation of carboxylic acids: kinetics and mechanistic interpretation

H.T. Gomes [a], J.L. Figueiredo [a], J.L. Faria [a,*], Ph. Serp [b], Ph. Kalck [b]

[a] *Laboratório de Catálise e Materiais, Departamento de Engenharia Química, Faculdade de Engenharia da Universidade do Porto, Rua Dr. Roberto Frias, 4200-465 Porto, Portugal*

[b] *Laboratoire de Catalyse, Chimie Fine et Polymères, Ecole Nationale Supérieure d'Ingénieurs en Arts Chimiques et Technologiques, 118 Route de Narbonne, 31077 Toulouse, France*

Received 2 July 2001; accepted 29 October 2001

Abstract

Carbon-supported iridium catalysts were prepared by different incipient wetness impregnation methods and by organometallic chemical vapor deposition. The catalysts were characterized by N_2 adsorption, TPD, SEM and H_2 chemisorption measurements. The results obtained indicate a clear dependency of the metal-phase dispersion on the pre-treatment of the carbon support and the impregnation method. Their activity for catalytic wet air oxidation of butyric and *iso*-butyric acid aqueous solutions was investigated in a stirred reactor at 473 K and 0.69 MPa of oxygen partial pressure. The conversions obtained after 2 h were 43 and 52%, with respect to each carboxylic acid, when the most active catalysts were used. The measured conversions and initial reaction rates correlate well with the exposed metal area. A rate equation was determined from measurements of the initial reaction rates at different oxygen partial pressures, temperatures and catalyst mass loads. The results were modeled considering a heterogeneously catalyzed free-radical mechanism.

Keywords: Catalytic wet air oxidation; Carbon-supported iridium catalysts; Incipient wetness impregnation; Organometallic chemical vapor deposition; Heterogeneous-catalyzed free-radical mechanism

1. Introduction

Wet air oxidation (WAO) is a useful process for reducing chemical oxygen demand (COD) of wastewaters, which can be used alone, or as pre-/post-treatment in combination with other processes, depending on the nature of the stream. In WAO, organic pollutants are usually mineralized to CO_2 and H_2O with an external oxidizing source (air or O_2) under conditions of high pressure and temperature [1–3].

Such conditions lead to very high investment costs, because reinforced materials are needed to support the strong pressures, and special metal alloys, which are much more expensive than commonly used stainless steel alloys, must be employed to avoid corrosion which is highly favored under these conditions. In spite of this, there has been a strong effort on the research and development of catalysts in order to bring down pressure and temperature to milder values—catalytic wet air oxidation (CWAO). Homogeneous catalysts such as copper [3–5] and iron salts [4] are

* Corresponding author. Tel.: +351-225-081-645/400; fax: +351-225-081-449.
E-mail address: jlfaria@fe.up.pt (J.L. Faria).

1381-1169/02/$ – see front matter
PII: S1381-1169(01)00475-7

very effective, but their use needs an additional separation step on the process, such as precipitation or membrane separation, to remove the catalyst from the final treated effluent.

As heterogeneous catalysts are easily removed from the liquid phase, very active catalysts were developed such as copper oxides supported on $ZnO–Al_2O_3$ [6–9], manganese–cerium [10] or cobalt–bismuth [5] composite oxides. But these catalysts also have a drawback, as toxic ions can leach to some extent into the solution, and therefore a further step is required to remove them. So, research on active and stable heterogeneous catalysts is fundamental. Carbon-supported noble metals are promising catalysts [11–13].

The use of iridium as the active phase in the preparation of supported metal catalysts has been somehow neglected. The existing reports concerning its application in CWAO are limited to some exploratory experiments, however with very promising results. One example is the ceria-supported iridium catalyst, with a good intrinsic activity (approx. $12\,mmol\,h^{-1}\,g_{cat}^{-1}$) in CH_3COOH oxidation [14]. A possible correlation between the activity of the metals and their chemical stability (in terms of their electrochemical potential, as defined in the Pourbaix diagrams [15]) has been established, and the ability of iridium to remain in the immunity domain in the reactant mixture recognized [14]. Recently, we have shown that carbon-supported iridium catalysts are also very active in the oxidation of butyric acid [16] and the present work gives complementary information on this type of catalysts.

Low molecular weight carboxylic acids (especially acetic acid) are very refractory compounds, being the end products of the degradation of several compounds. Therefore, research on the CWAO of low molecular weight carboxylic acids is of great importance. WAO of several acids including formic and acetic [17,18], glyoxalic and oxalic [18,19] and $C_3–C_5$ simple carboxylic acids [20–23] has been carried out. These studies contain very important information on the kinetics [17–22,24] and on the reaction mechanism [23]. Total oxidation of acetic acid was obtained with ruthenium supported on different materials [12,14,24], but the mechanism of the degradation of this kind of compounds is not yet fully understood. In this work, we used butyric acid as a model compound to study the degradation mechanism of low molecular weight carboxylic acids in heterogeneous CWAO processes.

2. Experimental

2.1. Support pre-treatment

The support material used to prepare iridium catalysts consisted of activated carbon pellets (Norit ROX 0.8) modified by different thermal and oxidative treatments. In all cases, the support was previously washed with 2 N HCl for 12 h under reflux, then with water until neutrality (pH 6) of the rinsing waters and finally dried overnight at 383 K. The material obtained after this procedure could be used as such or could undergo two types of oxidative treatments: (i) a liquid-phase oxidation with HNO_3 under reflux for 3 h, followed by washing with water for 6 h and finally drying overnight at 383 K (to be used for preparation of the Ir/CN catalysts); (ii) a gas-phase oxidation with O_2 diluted in nitrogen for 10 h at 723 K (to be used for preparation of the Ir/CO catalysts). TPD tests were made to determine the surface oxygen contents in the prepared supports. In the TPD tests, a sample of the given support was placed in the sample holder and degassed under He flow. Then the temperature was ramped at $5\,K\,min^{-1}$ up to 1373 K while the partial pressures of CO and CO_2 were recorded by a quadrupole mass spectrometer (Spectramass) equipped with a data acquisition system (Dataquad). The point of zero charge (PZC) was determined by mass titration [25]. The results obtained by TPD and mass titration are given in Table 1. Textural characterization of the support was also made by N_2 adsorption isotherms at 77 K. The BET surface area (S_{BET}), micropore volume (W_0) and mesoporous surface area (S_{Meso}) were then determined from these data.

2.2. Catalyst preparation

Iridium catalysts were prepared by two different methods: incipient wetness impregnation and organometallic chemical vapor deposition (OMCVD).

Two different procedures were used in the preparation of iridium catalysts (5 wt.%) by the incipient wetness impregnation with aqueous solutions of $(NH_4)_3IrCl_6$. In the conventional procedure, the precursor solution was poured down onto the support in a single step, using the appropriate concentration to obtain a 5 wt.% (Ir/C-1). In the alternative procedure two solutions were used in successive steps, in order

Table 1
Total amounts of CO and CO_2 released in TPD experiments and electrostatic characterization of the supports

Support	CO (μmol g^{-1})	CO_2 (μmol g^{-1})	CO/CO_2	Total O_2 (μmol g^{-1})	PZC
Non-oxidized	472	106	4.45	342	9.0
HNO_3-oxidized	1215	428	2.84	1036	6.4
O_2-oxidized	3350	346	9.68	2021	3.9

to obtain the same load (5 wt.%, Ir/C-2). After each impregnation step, the catalysts were dried overnight at 383 K.

A previously described method was used for the preparation of Ir/C catalysts by OMCVD in a fluidized bed reactor [26]. The support material consisted of the same Norit ROX 0.8 carbon in non-oxidized and HNO_3-oxidized forms. The gas-phase impregnation over the fluidized carbon support was carried out in a Pyrex cylindrical reactor (35 mm of internal diameter), using an iridium precursor developed for this purpose $[Ir(\mu\text{-}S\text{–}C_4H_9)(CO)_2]_2$ [27]. The deposition temperature was 408 K. The precursor was vaporized during 3.5 h at 393 K under reduced pressure (60 Torr) in a stream of He.

The catalysts were heated in helium at 673 K for 2 h prior to reaction. Reduction was then carried out in a stream (25 cm^3 min^{-1}) of helium-diluted hydrogen (10 v/v) at 623 K for 3 h. Finally, the catalysts were flushed with helium at 623 K for 30 min.

In order to evaluate the effect of temperature on the reduction of the metal, one of the impregnated catalysts was not reduced and another was reduced at higher temperature (723 K).

The nomenclature and textural description of the supports and catalysts prepared are given in Table 2.

2.3. Catalyst characterization

The amounts of iridium on the catalysts before and after reaction were measured by a gravimetric combustion method described elsewhere [11], based on the analysis of the ash content of the catalyst support compared to the catalyst combustion residue. The metal loads of the catalysts prepared by the impregnation method were found to be rather consistent in all cases (5.1 ± 0.4)%. Due to a less accurate control, the catalysts prepared by the OMCVD method had metal loads of 4.0 and 2.8%, for Ir/C-CVD and Ir/CN-CVD, respectively.

Metal dispersion was measured by H_2 chemisorption at room temperature using an automatic analyzer Coulter Omnisorp 100 CX. Scanning electron microscopy (Jeol JCM-35C electron microscope)

Table 2
Textural characterization of the supports and Ir/C catalysts prepared by the incipient wetness impregnation method

Material[a]	Support pre-treatment	S_{BET} (m^2 g^{-1})	W_0 (cm^3 g^{-1})	S_{Meso} (m^2 g^{-1})
C	Non-oxidized	1053	0.405	113
CN	HNO_3-oxidized	1060	0.408	110
CO	O_2-oxidized	1349	0.537	162
Ir/C-1	Non-oxidized	1023	0.392	112
Ir/C-2(NR)	Non-oxidized	994	0.383	109
Ir/C-2	Non-oxidized	1007	0.385	104
Ir/C-2(723)	Non-oxidized	931	0.361	100
Ir/CN-1	HNO_3-oxidized	1024	0.396	106
Ir/CN-2	HNO_3-oxidized	1025	0.394	113
Ir/CO-2	O_2-oxidized	1302	0.525	157

[a] All catalysts were reduced at 623 K except when otherwise indicated in brackets; the number 1 or 2, refers to single- or two-step impregnation, respectively.

was used to characterize the morphology of iridium particles.

2.4. Oxidation procedure

CWAO studies were performed in a 160 cm^3 stainless steel high-pressure reactor coated with a glass liner to prevent severe corrosion problems, heated by an electronically controlled heating mantle and stirred with a magnetically driven stirrer. In each run, the reactor was loaded with 70 cm^3 of 5 g dm^{-3} carboxylic acid aqueous solution and the catalyst. Before starting the reaction, the reactor was flushed with nitrogen for 15 min and heated to the reaction temperature under continuous stirring (500 rpm), after what pressurization with air started and reaction time was set to be zero.

Reactions performed during 8 h at 0.69 MPa of oxygen partial pressure and 473 K were chosen as the standard operating conditions. Under these conditions, the oxygen excess relative to the stoichiometric demand for complete oxidation of BA and *iso*-BA is 37%. Samples (1 cm^3) were withdrawn periodically and analyzed by gas chromatography on a capillary column (DBWAXetr, 0.32 mm ID, 1 μm film).

The effect of the impeller speed on the rate of oxidation was studied separately for each acid. Under the standard conditions, speeds up to 750 rpm (the maximum allowed by the experimental apparatus) were applied in order to check for external mass transfer control effects.

The initial reaction rates were calculated from the curves giving the concentration of carboxylic acid as a function of time at low conversion. They were expressed in $mmol_{acid}\,h^{-1}\,g_{Ir}^{-1}$. The reaction orders with respect to oxygen and to catalyst load were determined by varying the oxygen partial pressure in the 0.69–1.39 MPa range and the amount of catalyst in the 0.4–1.2 g range, while the activation energy was obtained by varying the reaction temperature in the 453–493 K range. First-order kinetics with respect to the concentration of the carboxylic acid was confirmed experimentally for the initial 2 h of reaction.

Butyric acid $CH_3(CH_2)_2CO_2H$, *iso*-butyric acid $(CH_3)_2CHCO_2H$, propionic acid $CH_3CH_2CO_2H$ and acetic acid CH_3CO_2H (supplied by Riedel-de Haën) were analyzed chromatographically and found to contain no discernible impurities. *N*-Methylaniline $C_6H_5NHCH_3$ (98% Sigma–Aldrich) was used as a free-radical inhibitor in heterogeneous-catalyzed oxidation experiments.

3. Results and discussion

3.1. Preliminary experiments and catalyst characterization

The oxidation of butyric acid was first tested in the absence of any metal and/or carbon support. The reaction was run for 8 h under standard conditions of pressure and temperature and a conversion of 3.1% was obtained. The same experiment in the presence of the non-oxidized activated carbon gave a conversion of 5.1%. These values were considered negligible in terms of carboxylic acid degradation, when compared to those obtained in the presence of the metallic catalysts.

In a first set of screening experiments, several metals including iridium and platinum were tested for the CWAO of butyric acid under the standard conditions of 473 K and 0.69 MPa relative pressure of O_2. For a metal loading of 5 wt.%, using a non-oxidized carbon support, it was observed that Ir/C and Pt/C catalysts have the best performances, with 2 h conversions above 40% [16]. Initial oxidation rates are about 30 $mmol_{acid}\,h^{-1}\,g_{Ir}^{-1}$ for Ir/C and 43 $mmol_{acid}\,h^{-1}\,g_{Pt}^{-1}$ for Pt/C. The other catalysts are quite inactive relative to the bare support (0.03 $mmol_{acid}\,h^{-1}\,g_{C}^{-1}$).

A slightly different order of activity was reported previously for the CWAO of acetic acid with ceria-supported catalysts [14]. From electrochemical data, it was concluded that the most active catalysts correspond to those where the metal remains in the metallic form under reaction conditions.

On the other hand, it is clear that the electrochemistry of the carbon surface is strongly affected by the oxidation treatment, as the PZC decreases with the oxidation, the decrease being more notorious in the gas-phase oxidation (Table 1).

Previous studies have shown that oxidation with O_2 develops surface groups like phenol, carbonyl and quinone, while HNO_3 oxidation leads to a high concentration of carboxylic acid groups in addition to those mentioned. These results correlate well with the change in PZC (Table 1), because the total

concentration of oxygenated groups increases from the non-oxidized to the gas-phase oxidized support, and most of these groups are acidic.

As expected, there is no marked difference in the textural properties of the catalyst in relation to the support. A slight decrease of the surface area, consistent in all measurements (Table 2), is due to the presence of the metallic phase.

As reported previously [28], gas-phase oxidation of the support leads to an enhancement of the porous structure (increase of micropore volume (W_0) and mesoporous surface area (S_{Meso})), while the liquid-phase oxidation does not change appreciably the existing textural properties.

3.2. Activity of the carbon-supported iridium catalysts

The performance of the iridium catalyst was found to be dependent on the method of preparation and pre-treatment used. The two-step incipient wetness impregnation produces a more active catalyst than the single-step incipient wetness impregnation or the OMCVD method (Table 3). Increasing the reduction temperature from 623 K (Ir/C-2(623)) to 723 K (Ir/C-2(723)) does not increase the initial activity. The most active catalyst is that prepared with the non-oxidized substrate using the two-step incipient wetness impregnation method.

From SEM studies, it is observed that Ir/C catalysts prepared by the two-step method produce agglomerates of smaller size than those prepared with the single-step method. The agglomerates are made of small globular particles of iridium. The mean diameter of the iridium particles can be estimated from the H_2 chemisorption measurements. These values were found to be 4.4 nm in the case of Ir/C-2 and 6.9 nm for Ir/C-1.

Since there are no marked differences between all the prepared catalysts from the textural point of view, the activity must be correlated with the exposed metal area. The interesting fact is that the dimension of the agglomerate is proportional to the concentration of the impregnation solution: the higher the concentration of the precursor solution (as in the single-step incipient wetness impregnation), the higher are the rate of nucleation and growth of iridium particles over the support.

Chemisorption measurements indicated a clear dependency of metal dispersion on the pre-treatment of the carbon used and impregnation method. As can be inferred from Table 3, there is an effect of the support pre-treatment on the dispersion of the metal phase, the values ranging from 16.2 to 25.2% for catalysts prepared by the two-step incipient wetness impregnation method and reduced at 623 K.

This observation is in line with SEM micrographs where particles in the sub-micrometer scale can be observed. However, particles tend to agglomerate in specific domains, not homogeneously distributed, with sizes ranging from 400 nm to 4 μm (Fig. 1).

In order to test the effect of the metal oxidation state on the reaction rate, the activities of the pre-reduced and pre-oxidized Ir/C were compared. Different pre-treatments of the Ir/C catalysts were

Table 3
Activity of the prepared Ir/C catalysts on the CWAO of butyric acid solutions

Catalyst	Dispersion (%)	Initial rate (mmol h^{-1} g^{-1})	Conversion after 2 h (%)
Ir/C-1	15.9	16.8	28.0
Ir/C-2(NR)	[a]	23.0	38.5
Ir/C-2	25.2	29.8	42.6
		31.1[b]	51.8[b]
Ir/C-2(723)	12.3	15.2	24.1
Ir/CN-1	17.8	13.9	24.8
Ir/CN-2	18.3	18.1	29.7
		15.1[b]	25.8[b]
Ir/CO-2	16.2	18.2	27.6
Ir/C-CVD	23.3	19.5	29.5
Ir/CN-CVD	21.3	8.9	9.5

[a] No value is given because the metal has not been previously reduced to the metallic form.
[b] CWAO of *iso*-butyric acid.

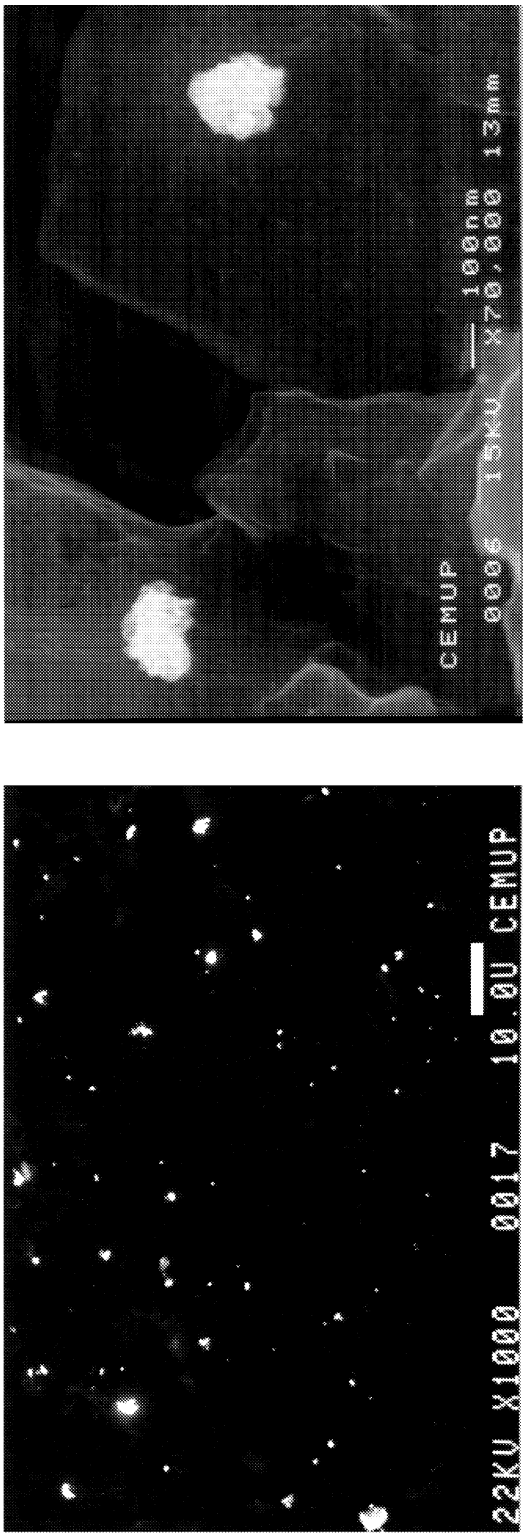

Fig. 1. SEM micrographs of the Ir/C-2 catalyst at different magnifications: (left) ×1000; (right) ×70 000.

Table 4
Activities of the Ir/C catalysts for butyric acid oxidation, after different pre-treatments

Catalyst	Expected metal state	Initial rate (mmol h^{-1} g^{-1})
Ir/C-2(NR)	Ir^{3+}	23.0
Ir/C-2(NR) oxidized at 298 K	Ir^{3+}	22.8
Ir/C-2(NR) oxidized at 623 K	Ir^{4+}	15.0
Ir/C-2	Ir^{0}	29.8
Ir/C-2 oxidized at 298 K	Ir^{0}–O_2	20.8
Ir/C-2 after reaction	Ir^{0}–O_2	18.6
Ir/C-2(723)	Ir^{0}	15.2

carried out before reaction and correspondingly different initial activities were measured (Table 4).

The most active catalyst is Ir/C-2, which has been reduced at 623 K. Oxidation of this catalyst at 298 K decreases considerably the initial rates of oxidation. The non-reduced catalyst Ir/C-2(NR) shows a reasonable activity, although less than that of the reduced catalyst. Oxidation of that catalyst at 298 K does not improve its activity. Increasing the oxidation temperature to 623 K decreases the rate even further. These results are well correlated with the increase in the oxidation state of the metal, confirming the importance of the metallic form (Ir^{0}) for catalytic activity.

Temperature should also be taken into account, because reduction at high temperatures (Ir/C-2(723)) gives a lower activity, possibly as result of metal sintering. It follows that the metal oxidation state is not the sole factor that influences the activity, temperature of reduction playing also an important role.

When the Ir/C-2(NR) catalyst is oxidized at a lower temperature (298 K) the activity is still significant, and comparable to the activity of the reduced catalyst when submitted to the same treatment (i.e. reduction at 623 K followed by oxidation at 298 K). This suggests that surface coverage by oxygen is sufficient to deactivate the catalyst. Two processes are taking place during the oxidation reaction: one concerns the oxidation of the metal surface, the other the competition of oxygen with the organic substrate for the active sites of the catalyst, indicating that the adsorption of the acid is the rate-controlling step. This result is in line with the fact that the reused catalyst (Ir/C-2 after reaction, in Table 4) loses activity due to poisoning of the surface by oxidation, which occurs during the degradation reaction. In fact, this surface oxygen coverage was confirmed by TPR in hydrogen atmosphere. During this experiment, hydrogen consumption occurred at 350 K, with desorption of water molecules. This is explained in terms of stoichiometric titration of surface oxygen.

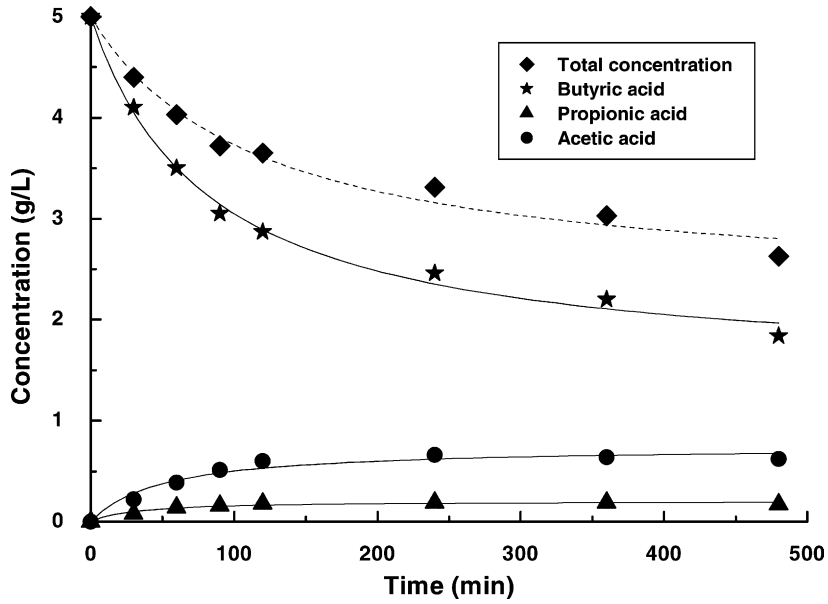

Fig. 2. CWAO of a butyric acid solution (57 mmol dm^{-3}) under standard conditions ($T = 473$ K, $P_{O_2} = 0.69$ MPa), using the Ir/C-2 catalyst.

Almost no consumption occurred at 583 K, which is the reduction temperature of iridium. The conclusion follows that iridium particles are not oxidized during the oxidation of butyric acid.

In Fig. 2, the change in composition of the reaction medium as a function of time under standard reaction conditions, using the Ir/C-2 catalyst, can be observed. Sixty-three percent of butyric acid conversion is obtained after 8 h, with 75% selectivity to CO_2, the remaining 25% being intermediate refractory compounds such as acetic and propionic acid. Acetone was also detected as an unstable intermediate that is readily converted to acetic acid. Other possible intermediate products, such as oxalic acid or formic acid, would be oxidized into CO_2 at very high rate under the present reaction conditions [13]. The initial rate of reaction was 29.8 mmol h^{-1} g_{Ir}^{-1}.

The disappearance of butyric acid was found to follow first-order kinetics in the first 2 h of reaction ($-dC_{But}/dt = k'C_{But}$).

The reaction does not seem to be sensitive to the structure of the substrate since for *iso*-butyric acid the kinetic curves and the corresponding values of initial rate are very similar to those of butyric acid (Table 3).

Fig. 3 shows the influence of the oxygen partial pressure on the initial rate of reaction, r_i. Measurements were taken at different pressures between 0.69 and 1.39 MPa of oxygen. The plot of $\ln(r_i)$ as a function of $\ln(P_{O_2})$ gives a straight line from which a 0.68 reaction order can be determined. This value compares with that obtained in the non-CWAO of acetic acid [20] under the same conditions (0.65) and the value reported with an Ir/C commercial catalyst [16] under similar conditions (0.61).

The observed dependency implies that the poisoning effect described previously in this section must be compensated somehow. Oxygen participation in the reaction mechanism cannot be limited to the adsorbed phase, as will be discussed in the following sections.

The influence of temperature was studied by running the reaction at 453, 473 and 493 K. From the Arrhenius-type plot of $\ln(r_i)$ as a function of $1/T$ (Fig. 4), an activation energy of 59.0 kJ mol^{-1} was measured. This value is roughly half of that obtained for WAO of acetic acid [12] under the same conditions (100.5 kJ mol^{-1}).

Measuring the initial butyric acid consumption rates for different amounts of 5%Ir/C catalyst in solution, an

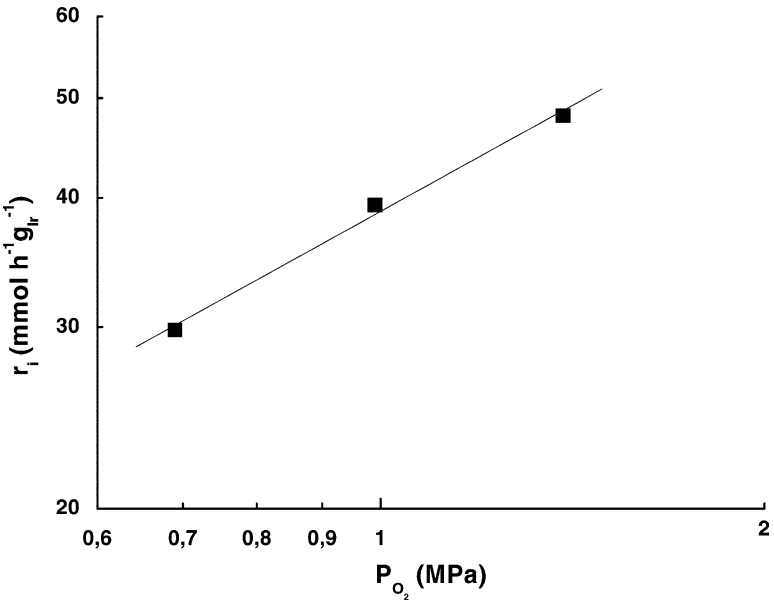

Fig. 3. Dependency of partial pressure of oxygen (MPa, log scale) on the initial rate (mmol h^{-1} g_{Ir}^{-1}) in the CWAO ($T = 473$ K) of a butyric acid solution (57 mmol dm^{-3}).

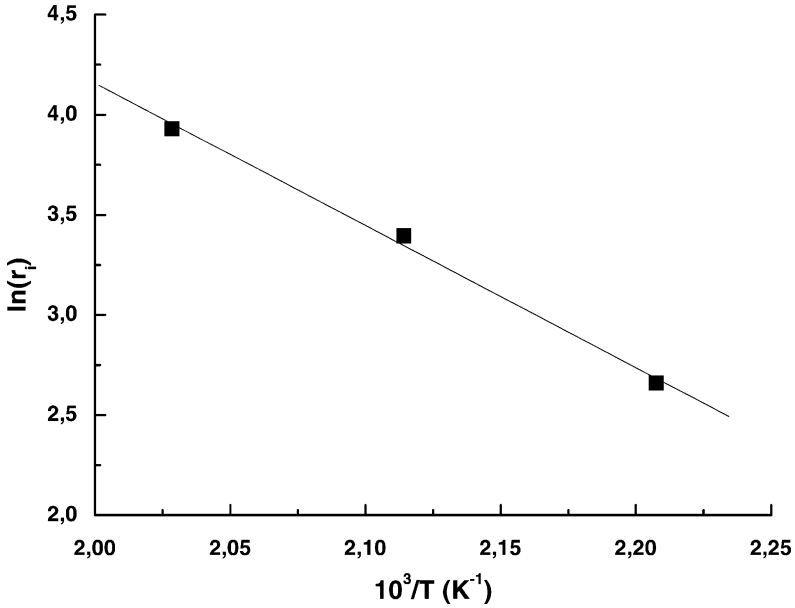

Fig. 4. Arrhenius-type plot (three temperature levels) for the butyric acid CWAO reaction over the Ir/C catalyst $P_{O_2} = 0.69$ MPa.

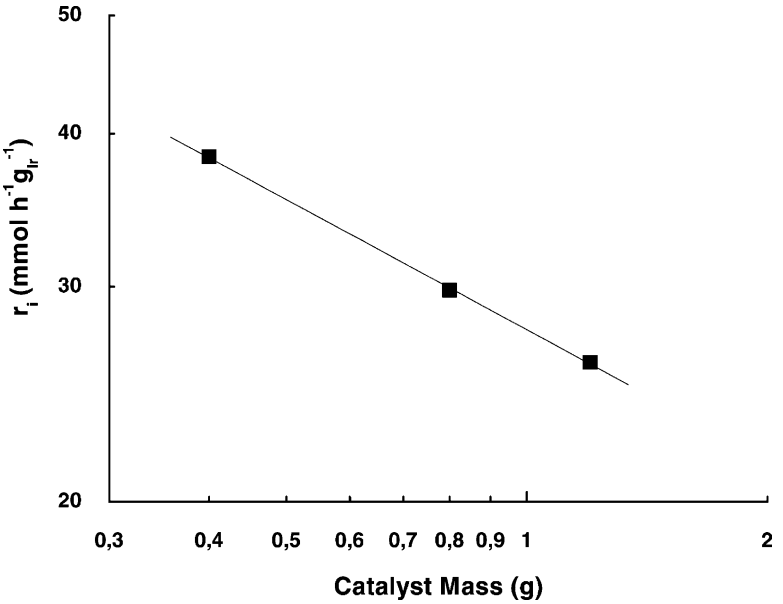

Fig. 5. Influence of catalyst mass on the rate of the 5 wt. %Ir/C catalyst at standard conditions ($T = 473$ K, $P_{O_2} = 0.69$ MPa, log scale).

order of −0.35 relative to this parameter was obtained (Fig. 5).

By combining these data, the initial rate of butyric acid oxidation (in mmol h^{-1} g_{Ir}^{-1}) can be expressed according to the rate equation

$$r_i = 1.8 \times 10^6 \, e^{-59\,000/RT} C_{But} P_{O_2}^{0.68} C_{Ir}^{-0.35} \quad (1)$$

with C_{But} in mmol dm^{-3}, P_{O_2} in MPa and C_{Ir} in g_{Ir} dm^{-3}. The validity of this equation has to be limited to the ranges of operating conditions used, which are $C_{But} = 57$ mmol dm^{-3}, 0.69 MPa $< P_{O_2} <$ 1.39 MPa, 0.29 g_{Ir} $dm^{-3} < C_{Ir} <$ 0.86 g_{Ir} dm^{-3} and 453 K $< T <$ 493 K.

3.3. Kinetic modeling of butyric acid CWAO

The experimental data obtained for the butyric acid CWAO over the Ir/C-2 catalyst at 473 K and 0.69 MPa oxygen partial pressure were modeled considering the reaction scheme presented in Fig. 6, where the reaction products propionic acid (Prop), acetic acid (Acet) and $CO_2 + H_2O$ are formed from butyric acid (But) via different paths. Propionic acid is considered to be converted into acetic acid and $CO_2 + H_2O$ and acetic acid is converted directly to the end products. The existence of different pathways was confirmed with independent studies of propionic and acetic acid oxidations under the same reaction conditions.

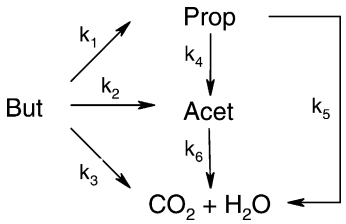

Fig. 6. Proposed scheme for butyric acid degradation.

The model employed was based on a Langmuir–Hinshelwood mechanism. It was assumed that the reaction occurs in the adsorbed state between an organic molecule and oxygen adsorbed dissociatively, characterized by adsorption equilibrium constants K_{But}, K_{Prop}, K_{Ace}, K_{O_2} and independent reaction rate constants k_i. It was also considered that competitive adsorption between the organic compounds and oxygen took place. With these assumptions, the butyric acid oxidation reaction can be described by the following set of differential equations:

$$-\frac{d[But]}{dt}\frac{1}{W} = \frac{(k_1 + k_2 + k_3) K_{But} [But] (K_{O_2}[O_2])^{1/2}}{(1 + K_{But}[But] + K_{Prop}[Prop] + K_{Ace}[Ace] + (K_{O_2}[O_2])^{1/2})^2} \quad (2)$$

$$\frac{d[Prop]}{dt}\frac{1}{W} = \frac{(k_1 K_{But}[But] - (k_4 + k_5) K_{Prop}[Prop])(K_{O_2}[O_2])^{1/2}}{(1 + K_{But}[But] + K_{Prop}[Prop] + K_{Ace}[Ace] + (K_{O_2}[O_2])^{1/2})^2} \quad (3)$$

$$\frac{d[Ace]}{dt}\frac{1}{W} = \frac{(k_2 K_{But}[But] + k_4 K_{Prop}[Prop] - k_6 K_{Ace}[Ace])(K_{O_2}[O_2])^{1/2}}{(1 + K_{But}[But] + K_{Prop}[Prop] + K_{Ace}[Ace] + (K_{O_2}[O_2])^{1/2})^2} \quad (4)$$

where K_{But}, K_{Prop}, K_{Ace} and K_{O_2} are adsorption equilibrium constants (dm^3 $mmol^{-1}$), k_i the reaction rate constants (mmol h^{-1} g_{Ir}^{-1}), [But], [Prop], [Ace] and $[O_2]$ are liquid-phase concentrations (mmol dm^{-3}) and W the metal concentration (g_{Ir} dm^{-3}).

The oxygen concentration in liquid phase was determined from the data published in the literature [29]. At a temperature of 473 K and for partial pressures of oxygen of 0.5, 1.5 and 2.5 MPa, the concentration of molecular O_2 in the liquid phase is, respectively, 6.69, 21.17 and 32.97 mmol dm^{-3}.

With the given data, a relationship between the oxygen partial pressure in the gas phase and the oxygen concentration in the liquid phase can be established:

$$[O_2] = 1.34314 P_{O_2} \quad (5)$$

On the other hand, the oxygen partial pressure in the gas phase decreases with time during the reaction. Taking into account, the total oxidation stoichiometries of each organic acid ((11), (13) and (14)), the oxygen concentration in the gas phase ($[O_2]_g$) changes

Table 5
Rate and adsorption equilibrium constants calculated upon application of the kinetic model

Rate constants (mmol h^{-1} g_{Ir}^{-1})						Adsorption constants (dm^3 $mmol^{-1}$)			
k_1	k_2	k_3	k_4	k_5	k_6	K_{But}	K_{Prop}	K_{Ace}	K_{O_2}
1.6×10^6	7.2×10^6	6.1×10^6	8.5×10^4	1.3×10^4	1.2×10^4	2.7×10^{-7}	3.1×10^{-5}	3.4×10^{-4}	6.2×10^{-3}

according to the oxygen mass balance relation:

$$[O_2]_g V_g = [O_2]_{g0} V_g - 5([But]_0 - [But]) V_l + 3.5[Prop] V_l + 2[Ace] V_l \quad (6)$$

with V_g and V_l being the gas-phase volume and liquid-phase volume, respectively, and $[O_2]_{g0}$ the initial oxygen concentration.

Under these conditions, ideal behavior of oxygen in the gas phase can be assumed without introducing a significant error, and thus

$$P_{O_2} = [O_2]_g RT \quad (7)$$

From Eqs. (5) and (7), a relationship between the oxygen concentration in the liquid phase and the oxygen concentration in the gas phase is obtained:

$$[O_2] = 0.0521[O_2]_g \quad (8)$$

Consequently, from Eq. (6) a relationship between the oxygen concentration in liquid phase and the organic acids concentrations is established.

This model was solved with the computational program MATLAB. In Table 5, the parameters that best-fit the experimental data of the butyric acid oxidation at 473 K and 0.69 MPa of oxygen partial pressure over catalyst Ir/C-2 are presented.

Fig. 7 shows that the model fits very well with the experimental results. The results are in line with the assumption that oxygen is more strongly adsorbed than the organic substrate. It also shows that the more refractory intermediates are more strongly adsorbed than the initial substrate, butyric acid. The rate of degradation of butyric acid is faster than that of propionic and acetic acids (the latter being very close).

The model developed does not take into account catalyst deactivation phenomena that might

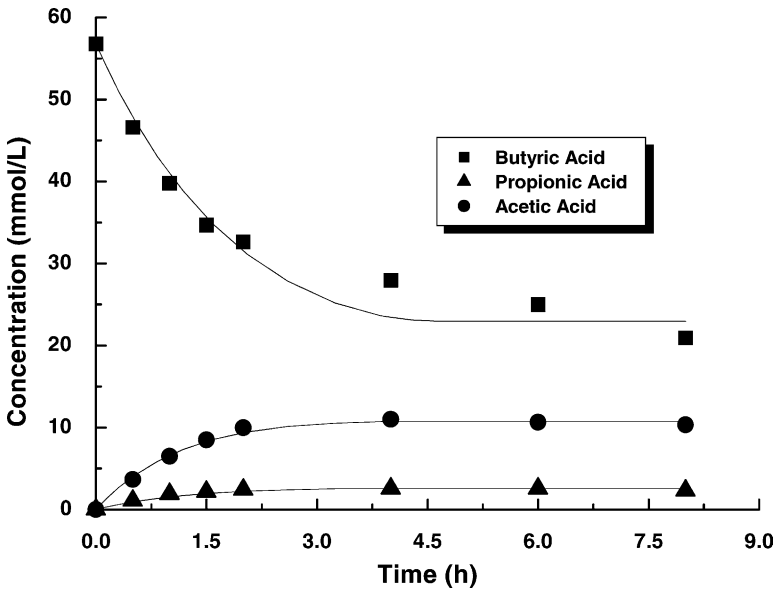

Fig. 7. Butyric acid oxidation reaction at 473 K over the Ir/C-2 catalyst. Comparison between the proposed kinetic model and the experimental results.

have occurred, explaining the discrepancies that can be observed between experimental and calculated data.

3.4. Mechanistic interpretation

Based on the above results, a conceptual mechanism for the CWAO of butyric acid can be proposed. The oxidative degradation of butyric acid to innocuous end products can be represented by the scheme given in Fig. 6. The reactions involved are:

$$CH_3CH_2CH_2COOH + \tfrac{3}{2}O_2 \xrightarrow{k_1} CH_3CH_2COOH + CO_2 + H_2O \quad (9)$$

$$CH_3CH_2CH_2COOH + 3O_2 \xrightarrow{k_2} CH_3COOH + 2CO_2 + 2H_2O \quad (10)$$

$$CH_3CH_2CH_2COOH + 5O_2 \xrightarrow{k_3} 4CO_2 + 4H_2O \quad (11)$$

$$CH_3CH_2COOH + \tfrac{3}{2}O_2 \xrightarrow{k_4} CH_3COOH + CO_2 + H_2O \quad (12)$$

$$CH_3CH_2COOH + \tfrac{7}{2}O_2 \xrightarrow{k_5} 3CO_2 + 3H_2O \quad (13)$$

$$CH_3COOH + 2O_2 \xrightarrow{k_6} 2CO_2 + 2H_2O \quad (14)$$

In order to establish a realistic pathway for the oxidation of butyric acid, we must account for the formation of the isolated intermediates, namely the propionic and acetic acids. Since the reaction occurs via heterogeneous catalysis, the primary step to be considered is the adsorption of both the carboxylic acid and molecular oxygen. The adsorption of both species in neighbor active sites will trigger the oxidation process by hydrogen abstraction from the α- or β-methyl units of the acid by O_2. This results in the formation of adsorbed organic radicals derived from the carboxylic acid and oxygen-derived reactive radicals such as hydroxyl ($HO^\bullet$) or hydroperoxyl ($HOO^\bullet$) radicals. All species will undergo fast desorption to generate free radicals in solution. The free radicals derived from the carboxylic acid substrate react with the dissolved O_2 to form peroxy radicals that can also abstract hydrogen from the carboxylic acid function of other molecules, leading to decarboxylation and production of CO_2. The peroxy radicals can also abstract hydrogen from the methyl groups of another molecule resulting in the formation of hydroperoxides and new free radicals (chain propagation reaction). The reaction continues until only the end products CO_2 and H_2O are formed:

$$C_3H_7CO_2H \rightleftarrows [C_3H_7CO_2H]_{ADS} \quad (15)$$

$$[C_3H_7CO_2H]_{ADS} + [\tfrac{1}{2}O_2]_{ADS} \rightarrow [{}^\bullet C_3H_6CO_2H]_{ADS} + [HO^\bullet]_{ADS} \quad (16)$$

$$[{}^\bullet C_3H_6CO_2H]_{ADS} \rightleftarrows {}^\bullet C_3H_6CO_2H \quad (17)$$

$${}^\bullet C_3H_6CO_2H + O_2 \rightarrow {}^\bullet OO\text{–}C_3H_6CO_2H \quad (18)$$

$${}^\bullet OO\text{–}C_3H_6CO_2H + C_3H_7CO_2H \rightarrow HOO\text{–}C_3H_6CO_2H + C_3H_6CO_2{}^\bullet \quad (19)$$

The hydroxyl and hydroperoxyl radicals react with the radicals derived from the carboxylic acid to generate the α- or β-hydroxy acid (as the primary step is α- or β-hydrogen abstraction) which is known [21] to lead to the formation of propionic and acetic acid under WAO conditions:

$$[HO^\bullet]_{ADS} \rightleftarrows HO^\bullet \quad (20)$$

$$CH_3C^\bullet HCH_2CO_2H + HO^\bullet \rightarrow CH_3C(OH)HCH_2CO_2H \quad (21)$$

$$CH_3C(OH)HCH_2CO_2H \xrightarrow{O_2} CH_3CO_2H + CO_2 + H_2O \quad (22)$$

$$CH_3CH_2C^\bullet HCO_2H + HO^\bullet \rightarrow CH_3CH_2C(OH)HCO_2H \quad (23)$$

$$CH_3CH_2C(OH)HCO_2H \xrightarrow{O_2} CH_3CH_2CO_2H + CO_2 + H_2O \quad (24)$$

Termination steps will occur when the free radicals formed undergo back hydrogen abstraction from another molecule in solution, thus leading to the starting carboxylic acid.

Now, the negative dependency of the initial rate on the amount of catalyst can be explained in terms of an heterogeneously catalyzed free-radical mechanism. Higher concentration of catalyst in the solution increases the rate of the initiation step, leading to higher concentration of radicals in solution, increasing the

rate of the termination step and consequently decreasing the reaction rate. To test this hypothesis, experiments were run in the presence of *N*-methylaniline. This compound works as a radical inhibitor, because of its ability to give away an hydrogen atom. In the present, *N*-methylaniline reacts easily with the carboxylic acid radicals, increasing the rate of the radical termination step. In fact, in the limit situation almost no conversion of butyric acid was observed in the presence of that radical scavenger.

In spite of the fact that butyric acid does not adsorb strongly on the iridium surface, hydrogen abstraction must occur at the metal surface (since the reaction in the presence of bare carbon is negligible), and the subsequent reaction proceeds via a long elementary chain reaction mechanism on the homogeneous liquid phase.

This also accounts for the observed reaction order for oxygen. Oxygen will act as a catalyst poison by covering the exposed metal surface. On the other hand, since it participates in the chain propagation reaction (Eq. (18)) in the homogeneous phase, a partial pressure increase will imply an increase of the specific rate of oxidation. The fact that the reaction order of oxygen is less than one already suggests that the oxygen contribution cannot be limited to a strongly adsorbed heterogeneous phase. Since the bimolecular reaction rates of oxygen with alkyl radicals in homogeneous phase have an order of magnitude of $10^9\,\mathrm{mol^{-1}\,dm^3\,s^{-1}}$ [30], it is natural to expect that this effect may overcome the catalyst poisoning.

Concerning an eventual contribution of external mass transfer control effects, it was observed that the activity did not depend on the stirring speed under the standard conditions. It was also checked that there was no internal diffusion control, because the activity of the catalyst did not change with the diameter of the catalyst particles in the range 200–800 μm. The activation energy values obtained are in line with the absence of any diffusional limitations.

Finally, from the standpoint of process engineering it should be noted that the formation of acetic acid in this reaction is a limitation because, in spite of –COOH being an electron-withdrawing group, the attack on the α position by electrophilic species (such as oxygen species) is very difficult, conferring an extremely refractory nature to this species.

4. Conclusions

1. Carbon-supported iridium catalysts proved to be very efficient systems in the CWAO of carboxylic acids, in particular when the metal is deposited on the support by the two-step incipient wetness impregnation method.
2. The catalyst activity was found to be dependent on the pre-treatment used. The initial reaction rates for butyric acid oxidation decreased with higher oxidation states of the iridium particles.
3. Oxygen coverage of the iridium surface decreases catalyst initial reaction rates. The first step of the reaction involves the adsorption of the organic molecule onto the metal surface, explaining the loss of activity due to the lowering of the adsorption coefficient of the substrate when the metal surface is highly covered by oxygen.
4. A kinetic study performed on a 5 wt.%Ir/C catalyst prepared by the two-step impregnation method led to the following empirical initial rate of oxidation of butyric acid ($\mathrm{mmol\,h^{-1}\,g_{Ir}^{-1}}$):

$$r_i = 1.8 \times 10^6\, \mathrm{e}^{-59\,000/RT} C_{\mathrm{But}} P_{\mathrm{O_2}}^{0.68} C_{\mathrm{Ir}}^{-0.35}$$

   with C_{But} is the butyric acid concentration ($\mathrm{mmol\,dm^{-3}}$), C_{Ir} the catalyst concentration ($\mathrm{g_{Ir}\,dm^{-3}}$) and $P_{\mathrm{O_2}}$ the oxygen partial pressure (MPa).
5. The experimental results were modeled considering Langmuir–Hinshelwood kinetics. The values obtained for the equilibrium adsorption constants show a clear contribution of oxygen adsorption on the iridium particles to the oxidation mechanism.
6. A heterogeneously catalyzed free-radical mechanism has been proposed. Adsorption of butyric acid and oxygen on neighbour iridium active sites triggers hydrogen abstraction from the organic substrate and initiates the chain reaction.

Acknowledgements

This work was carried out with support from Fundação para a Ciência e a Tecnologia (FCT) and Programa Operacional (POCTI), co-supported by FEDER (Project EQU/33401/99-00). Part of this work was supported by the Joint Programme

Ambassade de France au Portugal/ICCTI (Project 003/B3). HTG gratefully acknowledges FCT for his Ph.D. grant (PRAXIS XXI/BD/13498/97). The authors are indebted to Dr. Carlos Sá (CEMUP, Portugal) for the SEM analyses.

References

[1] V.S. Mishra, V.V. Mahajani, J.B. Joshi, Ind. Eng. Chem. Res. 34 (1995) 2.
[2] D. Mantzavinos, R. Hellenbrand, A.G. Livingston, I.S. Metcalfe, Appl. Catal. B 11 (1996) 99.
[3] S.H. Lin, S.J. Ho, Appl. Catal. B 9 (1996) 133.
[4] D. Mantzavinos, R. Hellenbrand, A.G. Livingston, I.S. Metcalfe, Appl. Catal. B 7 (1996) 379.
[5] S. Imamura, T. Sakai, T. Ikuyama, J. Jpn. Petrol. Inst. 25 (1982) 74.
[6] A. Pintar, J. Levec, Chem. Eng. Sci. 47 (1992) 2395.
[7] J. Levec, A. Pintar, Catal. Today 24 (1995) 51.
[8] A. Sadana, J.R. Katzer, Ind. Eng. Chem. Fundam. 13 (1974) 127.
[9] A.I. Njiribeako, R.R. Hudgins, P.L. Silveston, Ind. Eng. Chem. Fundam. 17 (1978) 234.
[10] S. Imamura, M. Nakamura, N. Kawabata, J. Yoshida, S. Ishida, Ind. Eng. Chem. Prod. Res. Dev. 25 (1986) 34.
[11] H.T. Gomes, J.L. Figueiredo, J.L. Faria, Appl. Catal. B 27 (2000) L217.
[12] P. Gallezot, S. Chaumet, A. Perrard, P. Isnard, J. Catal. 168 (1997) 104.
[13] P. Gallezot, N. Laurain, P. Isnard, Appl. Catal. B 9 (1996) L11.
[14] J. Barbier Jr., F. Delanoë, F. Jabouille, D. Duprez, G. Blanchard, P. Isnard, J. Catal. 177 (1998) 378.
[15] M. Pourbaix, Atlas of Electrochemical Equilibria in Aqueous Solutions, Cebelcor, Brussels, 1974.
[16] H.T. Gomes, J.L. Figueiredo, J.L. Faria, Catal. Today, (2002) in press.
[17] R.V. Shende, V.V. Mahajani, Ind. Eng. Chem. Res. 36 (1997) 4809.
[18] R.V. Shende, J. Levec, Ind. Eng. Chem. Res. 38 (1999) 3830.
[19] R.V. Shende, V.V. Mahajani, Ind. Eng. Chem. Res. 33 (1994) 3125.
[20] D.C. Day, R.R. Hudgins, P.L. Silveston, Can. J. Chem. Eng. 51 (1973) 733.
[21] P.E.L. Williams, P.L. Silveston, R.R. Hudgins, Can. J. Chem. Eng. 53 (1975) 354.
[22] R.V. Shende, J. Levec, Ind. Eng. Chem. Res. 38 (1999) 2557.
[23] N. Nikolaou, N. Abatzoglou, S. Gasso, E. Chornet, Can. J. Chem. Eng. 72 (1994) 522.
[24] J.-C. Béziat, M. Besson, P. Gallezot, S. Durécu, J. Catal. 182 (1999) 129.
[25] J.S. Noh, J.A. Schwarz, Carbon 28 (1990) 675.
[26] P. Serp, R. Feurer, R. Morancho, P. Kalck, J. Catal. 157 (1995) 294.
[27] P. Serp, R. Feurer, P. Kalck, H. Gomes, J.L. Faria, J.L. Figueiredo, Chem. Vap. Depos. 7 (2001) 59.
[28] A.E. Aksoylu, M.M.A. Freitas, J.L. Figueiredo, Appl. Catal. A 192 (2000) 29.
[29] K. Belkacemi, F. Larachi, S. Hamoudi, A. Sayari, Appl. Catal. A 199 (2000) 199.
[30] P. Neta, R.E. Huie, Mosseri, L.V. Shastri, J.P. Mittal, P. Maruthamuthu, S. Steenken, J. Phys. Chem. 93 (1989) 4099.